Highly interpenetrated diamondoid nets of Zn(II) and Cd(II) coordination networks from mixed ligands

Jian-Jr Cheng,[a] Ya-Ting Chang,[a] Chia-Jun Wu,[a] Yi-Fen Hsu,[a]
Chia-Her Lin,[a] Davide M. Proserpio*,[b] and Jhy-Der Chen*,[a]

[a]*Department of Chemistry, Chung-Yuan Christian University, Chung-Li, Taiwan, R.O.C.*

[b] *Universitá degli Studi di Milano , Dipartimento di Chimica Strutturale e Stereochimica Inorganica, , Via G.. Venezian 21, 20133 Milano, Italy*

Abstract

The synthesis, structures and thermal properties of three coordination networks [Zn($\mathbf{L}^1$)(1,4-BDC)] · H_2O ($\mathbf{L}^1$ = *N,N′*-di(4-pyridyl)adipoamide; 1,4-H_2BDC = 1,4-benzenedicarboxylic acid), **1**, [Cd($\mathbf{L}^1$)(1,4-BDC)] · 2H_2O, **2**, and [Zn_2($\mathbf{L}^2$)(1,4-BDC)$_2$] · 2CH_3OH ($\mathbf{L}^2$ = *N,N′*-di(4-pyridyl)dodecanamide), **3**, are reported. Complexes **1** and **2** show the **dia** topology with the rare 8- and 9-fold interpenetrating modes, respectively, while **3** exhibits an interpenetrating 3-fold framework with the **pcu** $Zn_2(COO)_2$ dimer decorated topology. Complex **2** shows the maximum number of interpenetration presently known for interpenetrating diamondoid networks of coordination networks containing mixed spacer ligands.

Introduction

Considerable effort has been devoted to understanding the self-assembly of organic and inorganic molecules in the past decade, because it extends the range of new solids which can be designed to have particular physical and chemical properties.[1,2] One of the most common nets observed in polymeric networks is related to the structure of diamond,[2] which is, in general, formed by propagating a tetrahedral nodal point in all four directions by coordinating a topological linear bidentate ligand. The diamondoid networks (**dia** using the 3-letter name)[3] are particularly intriguing because of their general 3D robustness, and are often involved in interpenetrating phenomena with a range from 2- up to 18-fold,[4] representing the largest class of interpenetrating nets in 3D coordination networks (30% according to a recent statistical analysis up to the year of 2009)[4(f)] The complex $[CuSO_4(\mathbf{L^1})(H_2O)_2]_\infty$ [$\mathbf{L^1}$ = *N,N'*-di(4-pyridyl)adipoamide] shows the highest degree of 12-fold interpenetration ever found for diamondoid nets exclusively based on coordination bonds,[5] while the 18-fold interpenetration of diamondoid frames was reported for the hydrogen-bonded complex prepared from the modular self-assembly of methanetetrabenzoic acid and 4,4'-bipyridine.[6] Diamondoid networks of coordination networks with mixed spacer ligands have been reported and the fold-interpenetrating number ranges from 2 to 8.[7]

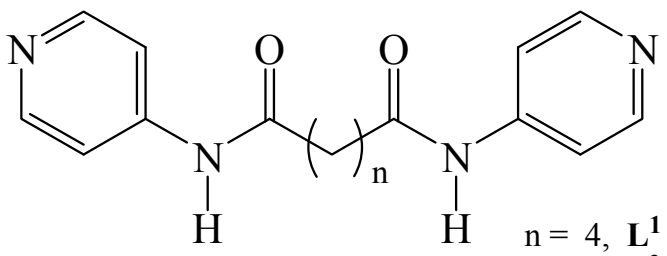

n = 4, $\mathbf{L^1}$
10, $\mathbf{L^2}$

The degree of interpenetration is strongly related to the length of the spacer ligand.[8] There are, however, other factors which can affect interpenetration, such as the bulkiness of the ligands and the counterions, the number and type of solvated molecules, the π-π interactions between the aromatic bridging ligands and the coordination geometry at the pseudotetrahedral centers.[8] In the complex $[CuSO_4(\mathbf{L^1})(H_2O)_2]_\infty$, combination of a long flexible ligand with a node located at the midpoint of dinuclear copper centers which are bridged by two SO_4^{2-} anions extended the degree of interpenetration.[5] Thus, the flexibility of the $\mathbf{L^1}$ spacer ligand as well as the diversities of geometrical arrangements of the metal centers are essential in determining the structural type.

To investigate the possibility of tuning the degree of interpenetration of coordination networks, we have reacted $\mathbf{L^1}$ and 1,4-H_2BDC (1,4-H_2BDC = 1,4-benzenedicarboxylic acid) with Zn(II) and Cd(II) salts, which afforded $[Zn(\mathbf{L^1})(1,4\text{-BDC})] \cdot H_2O$, **1**, and $[Cd(\mathbf{L^1})(1,4\text{-BDC})] \cdot 2H_2O$, **2**, showing 3D interpenetrating 8- and 9-fold distorted **dia** nets respectively. We have also synthesized the more flexible ligand *N,N′*-di(4-pyridyl)dodecanamide ($\mathbf{L^2}$) and reacted with 1,4-H_2BDC and Zn(II) salts, which afforded $[Zn_2(\mathbf{L^2})(1,4\text{-BDC})_2] \cdot 2CH_3OH$, **3**, showing a 3D 3-fold interpenetrating framework with a **pcu** $Zn_2(COO)_2$ dimer decorated topology. The syntheses, structures and thermal properties of these three complexes form the subject of this report.

Experimental section

General procedures

Elemental analyses were obtained from a PE 2400 series II CHNS/O analyzer or a HERAEUS VaruoEL analyzer. The IR spectra (KBr disk) were recorded on a Jasco FT/IR-460 plus spectrophotometer. Thermal gravimetric analyses (TGA) measurements were carried out on a TGA-2050 instrument at a scan rate of 10 ^{o}C/min. Powder X-ray patterns were recorded on a Panalytical PW3040/60 diffractometer.

Materials

The reagents ZnI_2, $CdBr_2$, dodecanedipoyl chloride and 4-aminopyridine were purchased from Aldrich Chemical Co.. The ligand *N,N′*-di(4-pyridyl)adipoamide (**L**^{1}) was prepared according to published procedures.[5,9]

N,N'-di(4-dipyridyl)dodecanedipoamide (L^{2})

Dodecanedipoyl chloride (1.46 g, 5.47 mmol) was slowly added to a DMF solution of 4-aminopyridine (1.03 g, 10.94 mmol). The mixture was stirred for 15 min and then triethylamine (1.11 g, 10.94 mmol) was added slowly. The mixture was refluxed for 6 h and then the volume was reduced to 10 ml by vacuum evaporation. A light yellow precipitate was obtained from the solution after standing at room temperature for 24 h. The solid was filtered off and washed with excess cold water and white powder was obtained. Yield: 1.78 g (85 %). ^{1}H NMR (DMSO-D_6, ppm): 10.27 (2H), 8.38 (4H), 7.54 (4H), 2.32 (4H), 1.55 (4 H), 1.62 (12H). Anal Calcd for $C_{24}H_{38}N_4O_4$: C, 64.55; H, 8.58; N, 12.55 %. Found: C, 64.50; H, 8.60; N, 12.58 %. IR (KBr disk, cm^{-1}): 3308(w), 3074(br), 1698(s), 1593(br), 1511(s), 1416(s), 1296(s), 1209(s), 949(m), 824(s), 518(s).

Preparation of [Zn(L^1)(1,4-BDC)] · H_2O, (1)

ZnI_2 (0.062 g, 0.20 mmol), 1,4-H_2BDC (0.034 g, 0.20 mmol) and **L^1** (0.06 g, 0.20 mmol) were placed in a in Teflon-lined digestion bomb (internal volume of 23 mL) containing 10 mL NaOH (0.04 M) solution under autogenous pressure. The reaction mixture was then heated at 120 °C for 2 days followed by slow cooling at 6 °C h^{-1} to room temperature. The colorless crystals were then collected, washed with water and then dried under vacuum. Yield: 0.043 g (39 %). Anal Calcd for $C_{24}H_{24}N_4O_7Zn$ (MW = 545.84): C, 51.95; H, 4.54; N, 10.09 %. Found: C, 51.91; H, 4.46 %; N, 9.66. IR (KBr disk, cm^{-1}): 3512(w), 3345(w), 3253(w), 3166(w), 3073(w), 3006(w), 2948(w), 1713(m), 1599(s), 1511(s), 1434(s), 1387(s), 1975(s), 1160(m), 1069(w), 1025(m), 836(m), 563(w), 527(w).

Preparation of [Cd(L^1)(1,4-BDC)] · $2H_2O$, (2)

Prepared as described for **1**, except that $CdBr_2$ (0.054 g, 0.2 mmol) was used. Yield: 0.082 g (67 %). Anal Calcd for $C_{24}H_{26}CdN_4O_8$ (MW = 610.89): C, 46.50; H, 4.39; N, 9.03 %. Found: C, 46.35; H, 4.40 %; N, 9.24. IR (KBr disk, cm^{-1}): 3521(m), 3262(m), 3082(w), 3013(w), 2932(w), 1707(m), 1596(s), 1559(s), 1510(s), 1462(w), 1428(s), 1387(s), 1333(s), 1305(m), 1247(w), 1210(m), 1154(m), 1017(m), 842(s), 747(m), 527(w).

Preparation of [Zn_2(L^2)(1,4-BDC)$_2$] · $2CH_3OH$, (3)

Prepared as described for **1**, except that **L^2** (0.077 g, 0.20 mmol) and 1,4-H_2BDC (0.034 g, 0.20 mmol) in 5 mL methanol and 5 mL H_2O were used. Yield: 0.040 g (11.0 %). Anal Calcd for $C_{40}H_{46}N_4O_{12}Zn_2$ (MW = 905.55): C, 52.57; N, 5.78; H, 5.34 %. Found: C, 53.05; N, 6.19; H, 5.12

%. IR (KBr disk, cm^{-1}): 3569 (w), 3560 (w), 3249 (w), 3164 (w), 3068 (w), 2997 (w), 2935 (w), 1720 (m), 1596 (s), 1510 (s), 1391 (s), 1151 (m), 1066 (s), 1032 (m), 835 (m), 549 (w), 526 (w).

X-ray crystallography

Single crystal X-ray diffraction data were collected on a Bruker APEX2 diffractometer (complexes **1** and **3**) or on a Bruker AXS P4 diffractometer (complex **2**), which were equipped with a graphite-monochromated Mo K_α ($\lambda_{K\alpha}$ = 0.71073 Å) radiation. Data reduction was carried by standard methods with use of well-established computational procedures.[10] The structure factors were obtained after Lorentz and polarization corrections. The positions of the heavy atoms, including the Zn and Cd atoms, were located by the direct method. The remaining atoms were found in a series of alternating difference Fourier maps and least-square refinements,[11] while the hydrogen atoms were added by using the HADD program and refined using a riding model. The C(8) and C(9) atoms of **1** are disordered such that two positions for each atom can be found. Basic information pertaining to crystal parameters and structure refinement is summarized in Table 1.

Results and Discussion

Structure of 1

Fig. 1(a) shows the coordination environment about the Zn(II) metal center. Selected bond distances and angles are listed in Table 2. The Zn(II) cation is four-coordinated by two nitrogen atoms from two $\mathbf{L^1}$ ligands and two oxygen atoms from two μ_1-η^1:η^0-monodentate 1,4-BDC^{2-} ligands

with Zn-N distances of 2.053(2) and 2.054(2) Å and Zn-O distances of 1.932(2) and 1.989(2), respectively. The other two Zn-O distances to O(4) and O(5A) are 2.562(2) and 3.021(2) Å, respectively, which are beyond the limit (2.5 Å)[12] that was counted as bidentate coordination, but the value of 2.562(2) Å is shorter than would normally occur in a van der Waals contact (2.91 Å).[13] The angles about the Zn(II) cation are in the range 95.61(9) – 126.08(10)°, indicating a distorted tetrahedral geometry. A single adamantanoid cage is illustrated in Fig. 1(b), which exhibits maximum dimensions of 38.56 x 29.28 x 17.68 $Å^3$. The Zn(II) adjoining nodes are separated by two different distances that are 19.49 (through $\mathbf{L^1}$) and 10.93 (through 1,4-BDC^{2-}) Å. The $\mathbf{L^1}$ ligand adopts the AGA *cis* conformation[14] and the dihedral angle between the two pyridyl rings is 65.72°, i.e. the two rings are twisted about the C-N bonds. Eight independent equivalent cages interpenetrate in the crystal structure by self-clathration grouping in two sets of four along the a-axis and related by a center of inversion, Fig. 1(c): this is a typical example of class IIIa of interpenetration with $Z_t = 4$ (down [1 0 0] separated from each other by 8.37 Å) and $Z_n = 2$ (inversion center). This is easily shown using the program package TOPOS.[15] Each **dia** framework supports hydrogen bonding through the uncoordinated water molecules [one N-H---O with N---O = 2.814 Å and two O-H---O with O---O = 2.646 and 2.794 Å, Fig. 1(d)], resulting in a single complicated multinodal net. There is no π-π interaction between the different nets. Due to the 8-fold interpenetration, the solvent-accessible volume is small and approximately 121.7 $Å^3$ (4.9 % of the unit cell) as calculated using the PLATON program.[16] For comparison, it is noted that in the 8-fold interpenetrated 3D **dia** net

observed for Zn(L)(1,4BDC) [L = *N,N'*-bis(4-pyridyl)phthalamide], no solvent-accessible volume was found in the structure.[7(q)]

Structure of 2

Fig. 2(a) shows the coordination environments about the two Cd(II) metal centers. The Cd(II) cation is six-coordinated by two nitrogen atoms from two $\mathbf{L^1}$ ligands and four oxygen atoms form two μ_1-η^1:η^1-chelating 1,4-BDC^{2-} ligands with Cd-N distances of 2.267(2) and 2.298(2) Å and Cd-O distances of 2.232(2) - 2.613(2) Å. The angles about the Cd(II) cation are in the range 52.56(7) – 143.20(7)°, indicating a highly distorted octahedral geometry for the Cd(II) center. A single adamantane cage is illustrated in Fig. 2(b), which exhibits maximum dimensions of 37.17 x 33.50 x 18.05 $Å^3$. The Cd(II) adjoining nodes are separated by two different distances that are 21.22 and 21.12 (through $\mathbf{L^1}$) and 11.26 and 11.16 (through 1,4-BDC^{2-}) Å. The $\mathbf{L^1}$ ligand adopts the AAA *trans* conformation[14] and the dihedral angle between the two pyridyl rings is about 0°. This conformation gives a longer ligand compared to **1**, hence more nets can interpenetrate: nine independent equivalent **dia** nets interpenetrate along the a-axis, Fig. 2(c). It belongs to class Ia interpenetration with Z_t = 9 and a single translational vector relates all nine nets: [1 0 0] with a separation from each other by 9.08 Å. Up to now only 5 examples of 9-fold **dia** nets are known.[4a,f] The nine frameworks are all crossed into a single complicated multinodal net by the hydrogen bonding interactions of the two uncoordinated water molecules via two N-H---O (N---O = 2.915 and 2.962 Å) and three O-H---O (O---O = 2.708, 2.913 and 2.963 Å) hydrogen bonds, Fig. 2(d). Short π-π contacts of 3.55 and 3.60 Å between the pyridyl rings of the **L** ligands in the different nets are also observed. The solvent-accessible volume is only 76.9 $Å^3$ and the

volume ratio was calculated to be 6.2 % using the PLATON program.

Structure of 3

Fig. 3(a) depicts a coordination environment about the $Zn_2(COO)_2$ dimer. The Zn(II) cation is four-coordinated by one nitrogen atom from one $\mathbf{L^2}$ ligand and three oxygen atoms from one μ_1-η^1:η^0-monodentate and one μ_2-η^1:η^1-bridging 1,4-BDC^{2-} ligands with Zn-N distances of 1.995(2) Å and Zn-O distances of 1.923(2) - 1.981(2) Å, respectively. The angles about the Zn(II) cation are in the range 97.54(8) – 121.93(8)°, indicating a distorted tetrahedral geometry. The Zn(II) atoms forms a dimer via the bridging (COO) of the 1,4-BDC^{2-} ligand with a metal separation of 3.47 Å. The $\mathbf{L^2}$ ligand adopts the AAGAAAGAA *trans* conformation[14] and the dihedral angle between the two pyridyl rings is 0°. If we take the dimer as the node of the net (the so called "cluster" representation)[4f], each dimer is joined to six other dimers via four 1,4-BDC^{2-} and two $\mathbf{L^2}$ and the final net will be 6-coordinated. The crystal structure of **3** reveals that the new phase consists of a 6-coordinated primitive cubic (**pcu**) 3-fold interpenetrated framework, Fig. 3(b). The different interpenetrated nets are connected by the N-H---O (N---O = 2.869 Å) hydrogen bonds, while the methanol molecules interact with the 1,4-BDC^- ligands through the O-H---O (O---O = 3.169 Å) hydrogen bonds, Fig. 3(c). There is no π-π interaction between the different nets. If we keep as nodes the 4-coordinated Zn and the bridging 1,4-BDC^{2-} ligands we get the "standard" representation[4f] as binodal 4-connected **mog** (moganite) type topology with point symbol of $(4.6^4.8)_2(4^2.6^2.8^2)$.[17] A schematic drawing for this topology is shown in Fig. S1 as supplementary materials. With both descriptions, obviously, we get the same kind of interpenetration with the three independent nets related by a single translation (down a-axis [1 0 0] and separated by 9.25 Å) hence of class Ia. The

solvent-accessible volume is approximately 129.3 $Å^3$ and the volume ratio was calculated to be 12.7 % using the PLATON program.

Thermal properties

The thermal gravimetric analyses (TGA) curves, Fig. S2, show that both complexes **1** and **2** are stable up to 40 °C. A total weight loss of 3.24 % and 6.44 % occurred in the temperature ranges 40 - 110 °C and 40 - 125 °C for **1** and **2**, respectively, presumably due to the removal of the water molecules per formula unit (calcd. 3.30 % for **1** and 5.89 % for **2**). While a weight loss of 30.50 % occurred in the temperature range 316 - 360 °C, corresponding to the removal of 1,4-BDC^{2-} ligands per formula unit (calcd. 30.07 %) and a weight loss of 49.63 % occurred in the temperature range 360 - 600 °C, corresponding to the removal of $\mathbf{L^1}$ ligands per formula unit (calcd. 51.73 %) for **1**, a weight loss of 72.28 % occurred in the temperature range 325 - 590 °C, corresponding to the removal of 1,4-BDC^{2-} and $\mathbf{L^1}$ ligands per formula unit (calcd. 73.09 %) was observed for **2**. Finally, the residual product weight of 15.93 % was found in the temperature after 600 °C, corresponding to the formation of ZnO (calcd. 14.91 %) for **1** and the residual product weight of 21.28 % was found in the temperature after 590 °C, corresponding to the formation of CdO (calcd. 21.02 %) for **2**. The TGA curve shows that **3** is stable up to 40 °C. A total weight loss of 6.83 % occurred in the temperature range 40 - 330 °C, presumably due to the removal of the two CH_3OH molecules per formula unit (calcd. 7.08 %). A weight loss of 41.95 % occurred in the temperature range 330 - 415 °C, corresponding to the removal of $\mathbf{L^2}$ ligands per formula unit (calcd. 42.24 %). Another weight loss of 33.02 % occurred in the temperature range 415 - 730 °C, corresponding to the removal of 1,4-BDC^{2-} ligands per formula unit (calcd. 32.71 %). Finally, the residual product weight of 18.20 % was

found in the temperature after 730 °C, corresponding to the formation of ZnO (calcd. 17.97 %).

To investigate the thermal stability of **1** and **2** upon removal of the cocrystallized water molecules, we have measured their variable temperature powder X-ray diffraction patterns from 30 to 170 ^{o}C, which show significant changes both in peak positions and intensities, Fig. S3(a)-(b). When the sample of **1** was heated to 130 °C, obvious changes in peak positions indicate the formation of the second phase. Interestingly, when the dehydrated sample pretreated at 130 °C was exposed to water vapor for one hour, the original crystalline phase of **1** was regenerated, Fig. 4. Similar phenomena were observed for **2**. When the dehydrated sample pretreated at 150 °C was exposed to water vapor for one hour, the original crystalline phase of **2** was also regenerated, Fig. 5. In marked contrast to **1** and **2**, the variable temperature powder X-ray diffraction patterns of **3** from 30 to 300 °C show no obvious changes, indicating that the framework remains rigid upon removal of methanol molecules, Fig. S3(c).

Conclusions

The synthesis, structures and thermal properties of three interpenetrated coordination networks from mixed ligands have been successfully accomplished. The diamondoid complexes **1** and **2** show distorted cages with 8- and 9-fold interpenetrating modes. The asymmetry obviously derives from the very different $\mathbf{L^1}$ and 1,4-BDC^{2-} ligands that give a very distorted adamantane cages, and the different degree of interpenetration arises from the different conformations of $\mathbf{L^1}$. In marked contrast to the complex $[CuSO_4(\mathbf{L^1})(H_2O)_2]_\infty$ with a 12-fold interpenetration,[5] combination of a long flexible $\mathbf{L^1}$ ligand with a short rigid 1,4-BDC^{2-}

ligands reduced the number of interpenetration, indicating that the degree of interpenetration of diamondoid networks of coordination networks containing the $\mathbf{L^1}$ ligands may be tuned by changing the length of the dicarboxylate ligand. The nature of the metal center (size and geometry) also alters the degree of interpenetration. To our best knowledge, complex **2** show the maximum number of interpenetration presently known for interpenetrating diamondoid networks of coordination networks containing mixed spacer ligands.[4f] We have also shown in **3** that increasing the number of the backbone carbon atom of the neutral spacer ligand not only decreases the degree of interpenetration but also changes the structural type. The diamondoid complexes **1** and **2** show more flexible frameworks than **3** upon removal and addition of the solvent molecules.

Electronic supplementary information (ESI) available

The drawings showing the coordination environment of the Zn(II) center and the **mog** topology for **3** and the variable temperature power X-ray diffraction patterns of **1** – **3**. CCDC reference numbers 791960 - 791962.

Acknowledgment

We are grateful to the National Science Council of the Republic of China for support.

References.

1 (a) E. R. T. Tiekink and J. J. Vittal, *Frontiers in Crystal Engineering*, John Wiley & Sons, Ltd., England, 2006; (b) R. Robson, B. E. Abrahams, S. R. Batten, R. W. Gable, B. F. Hoskins and J. Lieu, *Supramolecular Architecture*, ACS publications, Washington, DC,

1992; (c) O. M. Yaghi, H. Li, C. Davis, D. Richardson and T. L. Groy, *Acc. Chem. Res.,* 1998, **31**, 474; (d) C. B. Aakeröy and K. R. Seddon, *Chem. Soc. Rev.,* 1993, 397; (e) M. Fujita and K. Ogura, *Coord. Chem. Rev.,* 1996, **148**, 249; (f) C. B. Aakeröy, N. R. Champness and C. Janiak, *CrystEngComm,* 2010, **12**, 22.

2 (a) M. J. Zaworotko, *Chem. Soc. Rev.,* 1994, **23**, 283; (b) D. M. L.Goodgame, D. A. Grachvogel and D. J. Williams, *Angew. Chem. Int. Ed.,* 1999, **38**, 153; (c) N. W. Ockwig, O. Delgado-Friedrichs, M. O'Keeffe and O. M. Yaghi, *Acc. Chem. Res.,* 2005, **38**, 176.

3 M. O'Keeffe, M. A. Peskov, S. J. Ramsden and O. M. Yaghi, *Acc. Chem. Res.,* 2008, **41**, 1782.

4 (a) V. A. Blatov, L. Carlucci, G. Ciani and D. M. Proserpio, *CrystEngComm,* 2004, **6**, 377; (b) I. A. Baburin, V. A. Blatov, L. Carlucci, G. Ciani and D. M. Proserpio, *J. Solid State Chem.,* 2005, **178**, 2452; (c) I. A. Baburin, V. A. Blatov, L. Carlucci, G. Ciani and D. M. Proserpio, *Cryst. Growth Des.,* 2008, **8**. 519; (d) I. A. Baburin, V. A. Blatov, L. Carlucci, G. Ciani and D. M. Proserpio, *CrystEngComm,* 2008, **10**, 1822; (e) S. R. Batten, *CrystEngComm*, 2001, **3**, 67; (f) E. V. Alexandrov, V. A. Blatov, A. V. Kochetkov and D. M. Proserpio, *CrystEngComm,* 2011, **13**, 3947.

5 Y.-F. Hsu, C.-H. Lin, J.-D. Chen and J.-C. Wang, *Cryst. Growth Des.,* 2008, **8**, 1094.

6 Y.-B. Men, J. Sun, Z.-T. Huang and Q.-Y. Zheng, *CrystEngComm,* 2009, **11**, 978.

7 See for example, 2-fold: (a) F. A. A. Paz and J. Klinowski, *Inorg. Chem.,* 2004, **43**, 3882; (b) J.-J. Wang, C.-S. Liu, T.-L. Hu, Z. Chang, L.-F.Li, C.-Y. Yan, P.-Q. Chen, X.-H. Bu, Q. Wu, L.-J. Zhao, Z. Wang and X.-Z. Zhang, *CrystEngComm,* 2008, **10**, 681; 3-fold: (c)

G.-H. Wang, Z.-G. Li, H.-Q. Jia, N.-H. Hu and J.-W. Xu, *Cryst. Growth Des.,* 2008, **8**, 1932; (d) J.-D. Lin, J.-W. Cheng and S.-W. Du, *Cryst. Growth Des.,* 2008, **8**, 3345; (e) W.-L. Zhang, Y.-Y. Liu, J.-F. Ma, H. Jiang and J. Yang, *Polyhedron,* 2008, **27**, 3351; (f) R. Mondal, M. K. Bhunia and K. Dhara, *CrystEngComm,* 2008, **10**, 1167; (g) Y. Lin, L. Zhang, J. Li and A. X. Hu, *Cryst. Growth Des.,* 2009, **9**, 2043; (h) K. O. Ashiry, Y.-H. Zhao, K.-Z. Shao, Z.-M. Su and G.-J. Xu, *Polyhedron,* 2009, **28**, 975; 4-fold: (i) J. Zhang, R. Liu, P. Feng and X. Bu, *Angew. Chem. Int. Ed.,* 2007, **46**, 8388; (j) H. Jiang, J. F. Ma, W.-L. Zhang, Y.-Y. Liu, J. Yang, G.-J. Ping and Z.-M. Su, *Eur. J. Inorg. Chem.,* 2008, 745; (k) X.-Q. Liang, X.-H. Zhou, C. Chen, H.-P. Xiao, Y.-Z. Li, J.-L. Zuo and X.-Z. You, *Cryst. Growth Des.,* 2009, **9**, 1041; 5-fold: (l) Y. Qi, Y.-X. Che and J.-M. Zheng, *Cryst. Growth Des.,* 2008, **8**, 3602; (m) K.-L. Huang, X. Liu and G.-M. Liang, *Inorg. Chim. Acta,* 2009, **362**, 1565; (n) Y.-W. Li, W.-L. Chen, Y.-H. Wang, Y.-G. Li and E.-B. Wang, *J. Solid State Chem.,* 2009, **182**, 736; (o) D. Liu, H.-X. Li, Y. Chen, Y. Zhang and J.-P. Lang, *Chin. J. Chem.,* 2008, **26**, 2173; (p) A. Aijaz, E. Barea and P. K. Bharadwaj, *Cryst. Growth Des.,* 2009, **9**, 4480; 8-fold: (q) Y. Gong, J. Li, J. Qin, T. Wu, R. Cao and J. Li, *Cryst. Growth Des.,* 2011, **11**, 1662.

8 L. Carlucci, G. Ciani, D. M. Proserpio and S. Rizzato, *Chem. Eur. J.*, 2002, **8**, 1520.

9 L. Rajput, S. Singha and K. Biradha, *Cryst. Growth Des.,* 2007, **7**, 2788.

10 (a) XSCANS, Release, 2.1, Siemens Energy & Automation, Inc, Madison, Wisconsin, USA, 1995; (b) *SMART/SAINT/ASTRO*, Release 4.03, Siemens Energy & Automation, Inc., Madison, Wisconsin, USA, 1995.

11 G. M. Sheldrick, *Acta Crystallogr.,* 2008, **A64**, 112.

12 M. M. Harding, *Acta Crystallogr., Sect. D,* 2006, **62**, 678.

13 A. Bondi, *Phys. Chem.,* 1964, **68**, 441.

14 H.-C. Chen, H.-L. Hu, Z.-K. Chan, C.-W. Yeh, H.-W. Jia, C.-P. Wu, J.-D. Chen and J.-C. Wang, *Cryst. Growth Des.,* 2007, **7**, 698; (b) Y.-F. Hsu, W. Hsu, C.-J. Wu, P.-C. Cheng, C.-W. Yeh, W.-J. Wang, J.-D. Chen and J.-C. Wang, *CrystEngComm,* 2010, **12**, 702.

15 http://www.topos.ssu.samara.ru; V. A. Blatov, *IUCr CompComm Newsletter,* 2006, **7**, 4.

16 A. L.Spek, *J. Appl. Cryst.,* 2003, **36**, 7.

17 V. A. Blatov, M. O'Keeffe and D. M. Proserpio, *CrystEngComm,* 2009, **11**, 44.

Table 1. Crystal data for **1** - **3**.

Complex	**1**	**2**	**3**
Formula	$C_{24}H_{24}N_4O_7Zn$	$C_{24}H_{26}CdN_4O_8$	$C_{40}H_{46}N_4O_{12}Zn_2$
Formula weight	545.84	610.89	905.55
crystal system	Monoclinic	Triclinic	Triclinic
space group	$P2_1/n$	$P\bar{1}$	$P\bar{1}$
a, Å	8.3732(4)	9.0807(15)	9.2535(2)
b, Å	19.2810(9)	11.3600(16)	10.2529(2)
c, Å	15.4445(7)	13.2607(19)	11.8897(3)
α, °	90	92.714(13)	91.372(1)
β, °	90.890(2)	106.281(16)	111.487(1)
γ, °	90	107.242(14)	102.427(1)
V, Å^3	2493.1(2)	1241.3(3)	1018.47(4)
Z	4	2	1
d_{calc}, g/cm^3	1.454	1.634	1.476
F(000)	1128	620	470
μ(Mo K□), mm^{-1}	1.036	0.936	1.245
limiting indices	$-11 \le h \le 11$, $-24 \le k \le 25$, $-20 \le l \le 20$	$-10 \le h \le 1$, $-13 \le k \le 13$, $-15 \le l \le 15$	$-12 \le h \le 12$, $-13 \le k \le 13$, $-15 \le l \le 15$
independent reflections	6229 [R(int) = 0.0565]	4384 [R(int) = 0.0258]	5029 [R(int) = 0.0524]
data / restraints / parameters	6229 / 0 / 343	4384 / 0 / 340	5029 / 0 / 253
quality-of-fit indicator [c]	1.006	1.071	1.085
final R indices[$I > 2\sigma(I)$] [a,b]	R1 = 0.0410, wR2 = 0.0950	R1 = 0.0236, wR2 = 0.0599	R1 = 0.0399, wR2 = 0.1245
R indices (all data)	R1 = 0.0886, wR2 = 0.1035	R1 = 0.0258, wR2 = 0.0612	R1 = 0.0492 wR2 = 0.1287

[a] $R_1 = \Sigma||F_o| - |F_c|| / \Sigma|F_o|$. [b] $wR_2 = [\Sigma w(F_o^2 - F_c^2)^2 / \Sigma w(F_o^2)^2]^{1/2}$.
$w = 1 / [\sigma^2(F_o^2) + (ap)^2 + (bp)]$, $p = [\max(F_o^2 \text{ or } 0) + 2(F_c^2)] / 3$.
a = 0.0419, b = 0.000 for **1**; a = 0.0229 , b = 0.6370 for **2**; a = 0.0802 , b = 0.0012 for **3**.
[c] quality-of-fit = $[\Sigma w(|F_o^2| - |F_c^2|)^2 / N_{observed} - N_{parameters})]^{1/2}$.

Table 2. Selected bond distances (Å) and angles (°) for **1** – **3**.

1			
Bond distances			
Zn-O(6A)	1.932(2)	Zn-O(3)	1.989(2)
Zn-N(4B)	2.053(2)	Zn-N(1)	2.054(2)
Bond angles			
O(6A)-Zn-O(3)	126.08(10)	O(6A)-Zn-N(1)	98.41(9)
O(3)-Zn-N(1)	119.65(9)	O(6A)-Zn-N(4B)	112.15(9)
O(3)-Zn-N(4B)	95.61(9)	N(1)-Zn-N(4B)	103.28(9)
2			
Bond distances			
Cd-O(6)	2.232(2)	Cd-N(1)	2.267(2)
Cd-O(3)	2.281(2)	Cd-N(3)	2.298(2)
Cd-O(4)	2.426(2)	Cd-O(5)	2.613(2)
Bond angles			
O(6)-Cd-N(1)	115.39(8)	O(6)-Cd-O(3)	134.17(8)
N(1)-Cd-O(3)	89.02(7)	O(6)-Cd-N(3)	89.77(8)
N(1)-Cd-N(3)	106.97(7)	O(3)-Cd-N(3)	120.95(8)
O(6)-Cd-O(4)	97.58(8)	N(1)-Cd-O(4)	143.20(7)
O(3)-Cd-O(4)	55.06(7)	N(3)-Cd-O(4)	88.10(7)
O(6)-Cd-O(5)	52.56(7)	N(1)-Cd-O(5)	89.90(7)
O(3)-Cd-O(5)	92.11(8)	N(3)-Cd-O(5)	142.25(7)
O(4)-Cd-O(5)	98.30(8)		
3			
Bond distances			
Zn-O(2)	1.923(2)	Zn-O(5A)	1.961(2)
Zn-O(4)	1.981(2)	Zn-N(1)	1.995(2)
Bond angles			
O(5A)-Zn-O(2)	121.93(8)	O(2)-Zn-O(4)	97.82(8)
O(5A)-Zn-O(4)	116.11(8)	O(2)-Zn-N(1)	115.49(9)
O(5A)-Zn-N(1)	97.54(8)	O(4)-Zn-N(1)	108.23(8)

Symmetry transformations used to generate equivalent atoms :

(A) x-1/2,-y+1/2,z+1/2 ; (B) x-3/2,-y-1/2,z-1/2 for **1**.

(A) -x+1,-y+1,-z+1 for **3**.

Captions

Fig. 1. (a) Coordination environment of the Zn(II) center in **1**. Symmetry transformations used to generate equivalent atoms: (A) x-1/2,-y+1/2,z+1/2; (B) x-3/2,-y-1/2, z-1/2; (C) x+1/2,-y+1/2,z-1/2; (D) x+3/2,-y-1/2,z+1/2. (b) A diagram showing a single adamantanoid cage. (c) A schematic view of the 8-fold interpenetration. (d) A drawing showing the N-H---O and O-H---O hydrogen bonds that connect the nets.

Fig. 2. (a) Coordination environment of the Cd(II) center in **2**. Symmetry transformations used to generate equivalent atoms: (A) –x+1,-y-1,-z+2; (B) -x-2,-y,-z; (C) -x,-y+1,-z+2; (D) -x+1,-y+1,-z+1. (b) A diagram showing a single adamantanoid cage. (c) A schematic view of the 9-fold interpenetration. (d) A drawing showing the N-H---O and O-H---O hydrogen bonds and the π-π interactions that connect the nets.

Fig. 3. (a) Coordination environment of the $Zn_2(COO)_2$ dimer in **3**. Symmetry transformations used to generate equivalent atoms: (A) -x+1,-y+1,-z+1. (b) A schematic view of the 3-fold interpenetration. (c) A drawing showing the N-H---O hydrogen bonds that connect the nets. The methanol molecules interact with the 1,4-BDC^- ligands through the O-H---O interactions.

Fig. 4. Powder XRD patterns of **1**. (a) simulated (b) at 30°C (c) at 130°C (d) heated to 130°C then exposed to water vapor.

Fig. 5. Powder XRD patterns of **2** (a) simulated (b) at 30°C (c) at 150°C (d) heated to 150°C then exposed to water vapor.

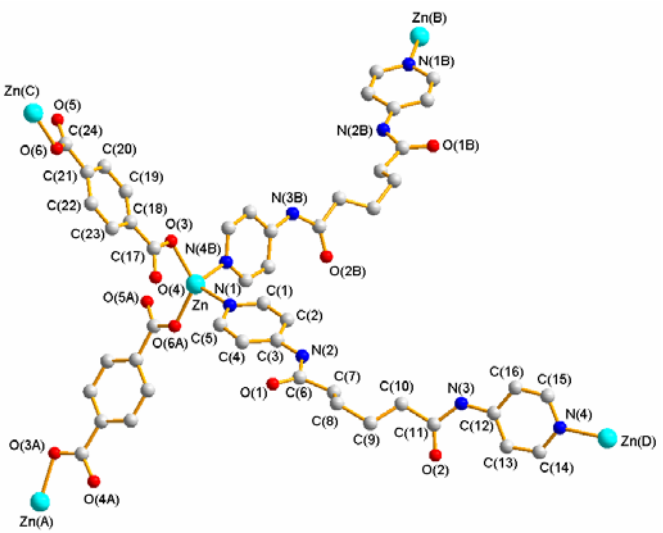
Zn(B)
N(1B)
N(2B)
O(1B)
Zn(C)
O(5)
C(24)
O(6)
C(20)
C(21)
C(19)
C(22)
C(18)
C(23)
O(3)
C(17)
N(4B)
N(3B)
O(2B)
O(4)
N(1)
C(1)
O(5A)
Zn
C(2)
O(6A)
C(5)
C(4)
C(3)
N(2)
O(1)
C(6)
C(7)
C(8)
C(10)
N(3)
C(16)
C(15)
C(9)
C(11)
C(12)
N(4)
Zn(D)
O(2)
C(13)
C(14)
O(3A)
O(4A)
Zn(A)

(a)

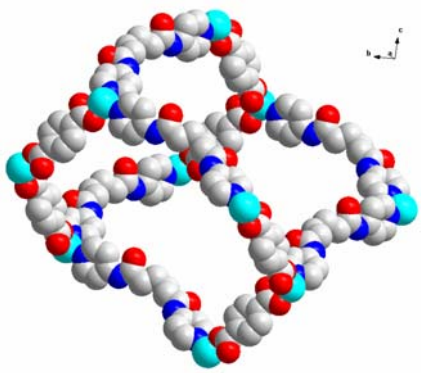

(b)

Fig. 1

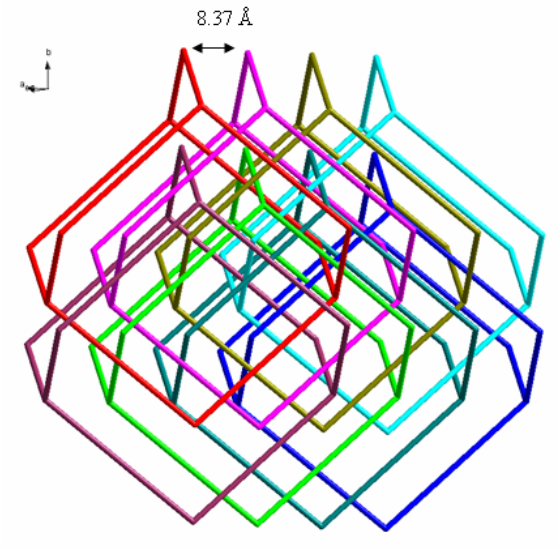

(c)

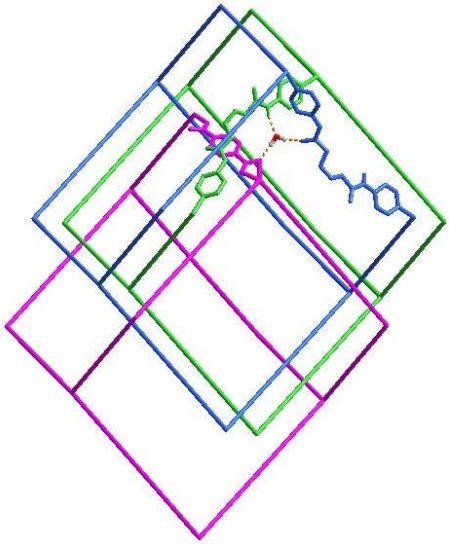

(d)

Fig. 1

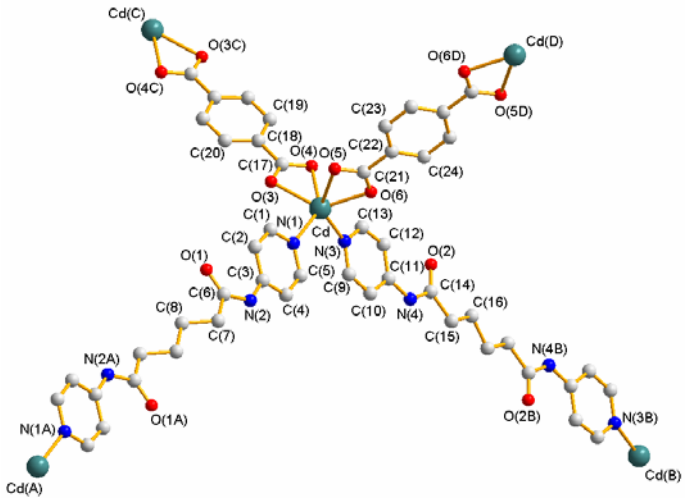
Cd(C)
O(3C)
O(4C)
C(19)
C(18)
C(20)
C(17)
O(4)
O(5)
C(22)
C(23)
O(6D)
Cd(D)
O(5D)
C(24)
C(21)
O(6)
O(3)
C(1)
N(1)
Cd
C(13)
C(2)
N(3)
C(12)
O(1)
C(3)
C(5)
C(11)
O(2)
C(6)
C(9)
C(14)
C(8)
N(2)
C(4)
C(10)
N(4)
C(16)
C(7)
C(15)
N(2A)
N(4B)
O(1A)
O(2B)
N(3B)
N(1A)
Cd(A)
Cd(B)

(a)

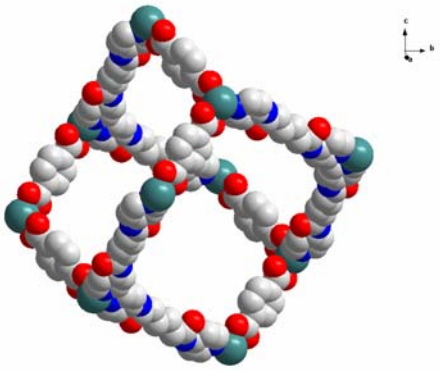

(b)

Fig. 2

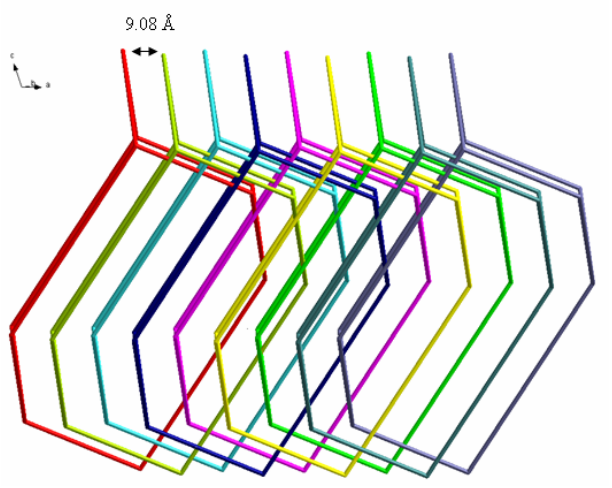

(c)

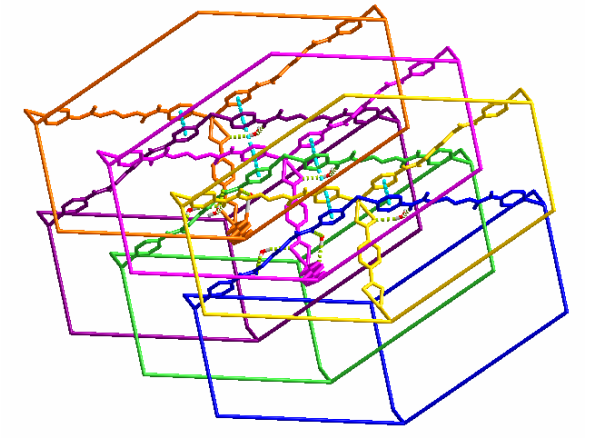

(d)

Fig. 2

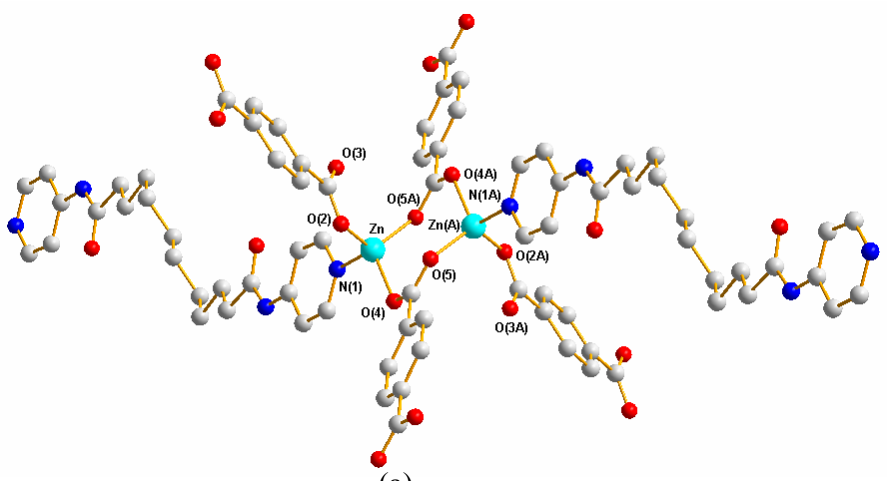

(a)

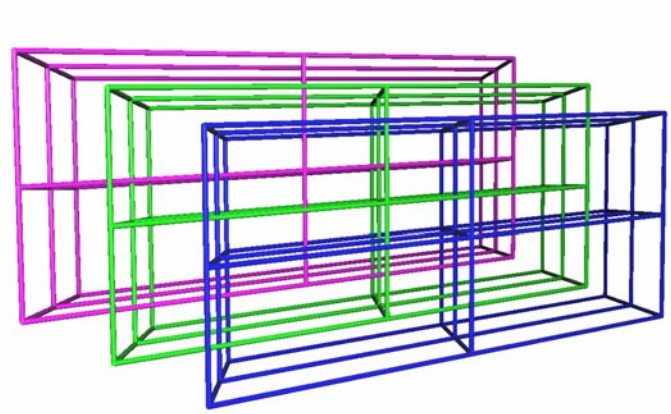

(b)

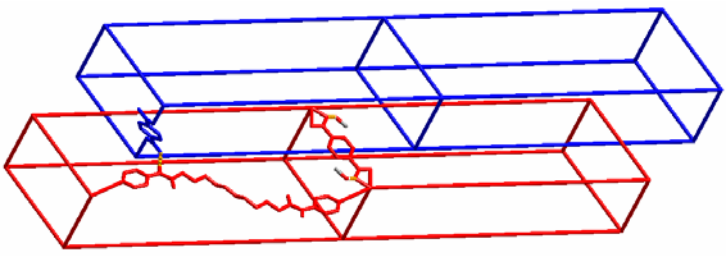

(c)

Fig. 3

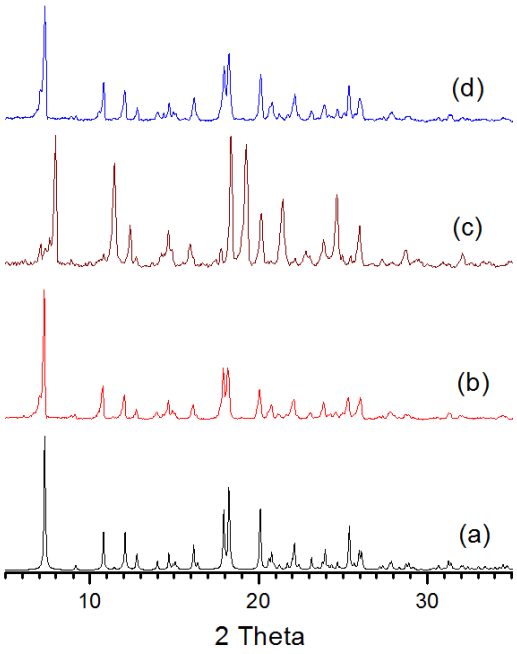

Fig. 4

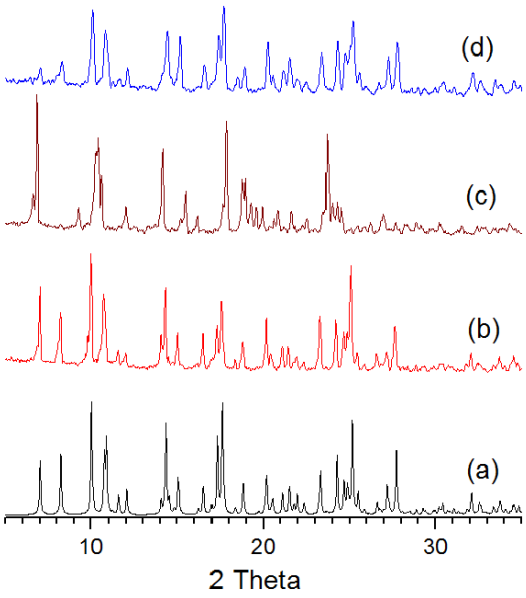

Fig. 5